https://doi.org/10.52326/ic-ecco.2021/EL.01

Nanoparticles as Building Units for Bio-Inspired Electronics –Switching and Sensing

Niko Carstens[1], Matteo Mirigliano[2], Thomas Strunskus[1], Franz Faupel[1], Oleg Lupan[2], Paolo Milani[3], Alexander Vahl[1,3]

[1] Institute for Materials Science, Chair for Multicomponent Materials, Kiel University, Kaiserstraße 2, 24143 Kiel, Germany

[2] Center for Nanotechnology and Nanosensors, Technical University of Moldova, 168 Stefan cel Mare Av., MD-2004 Chisinau, Republic of Moldova

[3] CIMAINA and Dipartimento di Fisica, Universita degli Studi di Milano, Via Giovanni Celoria 16, 20133 Milano, Italy

***Abstract*— Owing to their high surface-to-volume ratio, their small size and the high number of intrinsic defects, nanoparticless (NPs) exhibit properties that go beyond typical bulk materials. Consequently, nanogranular systems, with NPs as their fundamental building units, differ in many aspects from their atom-assembled counterparts. In this work, gas phase synthesis of NPs is applied as it offers the benefit of a high purity, surfactant free deposition that is compatible with a broad range of substrates. At the example of three fundamentally different NP assemblies it is showcased, how the unique properties of NPs make them promising building units for electronic devices with neuron-inspired functionalities. First, metal-insulator-metal structures with sparse embedding of AgAu alloy NPs inside a dielectric matrix are investigated for their diffusive memristive switching with distinct, well-separable resistance states. Secondly, the dynamic transitions between multiple resistance states in highly interconnected multi-terminal Ag NP networks are described. Lastly, illumination-dependent resistance states are investigated in two-terminal TiO_2 NP sensor devices.**

Keywords—nanoparticles; gas phase synthesis; sensors; memristive switching; nanoparticle networks; neuromorphic engineering

I. INTRODUCTION

The transformation towards a data driven society goes hand in hand with the rapid development of artificial intelligence and machine learning that enable the processing of the ever-increasing amount of big data. Despite the immense growth in the computational capabilities within the past decade(s), current technology still largely relies on silicon-based digital computers, that accommodate to contemporary highly parallel data processing tasks at the expense of power efficiency. Thus, novel, energy efficient device architectures and computing concepts are in high demand. A potential inspiration can be drawn from the earths most abundant, widely distributed computing devices – neuronal networks such as, e.g. the human brain. These systems have been evolutionarily optimized to accomplish highly robust, power efficient and adaptive information processing and can be found, in different variants and complexities, in organism throughout different scales. In contrast to digital computers, neuronal networks combine processing and memory at the local synaptic level and are arranged in highly parallel, dynamic networks.[1,2] Another striking feature of neuronal networks is the close connection of sensing (stimulus detection) and processing (data processing). The growing field of neuromorphic engineering draws inspiration from the features of neuron assemblies to engineer bio-inspired devices and circuits that are capable to perform complex tasks at high efficiency.[3]

Memristive devices with their intrinsic capabilities of memory and processing are often considered for the reproduction of synaptic features, such as spike time dependent plasticity and long-term potentiation.[4] Parallel crossbar arrays of memristive devices are frequently reported in applications in in-memory computing and hardware-based deep learning.[5–7] The unique electronic properties of memristive devices inspire applications that go beyond conventional electronics, e.g. to realize logics for in array computing or in neuromorphic engineering.[8] NPs have recently attracted attention as building blocks for memristive switching devices and are readily employed, either to enhance the reproducibility by tailoring the electrical field inside the dielectric matrix or to act as a source of mobile metallic cations.[9–12] Diffusive memristive switching, synonymously termed threshold switching, has been observed in a variety of devices with Ag or Ag-containing (alloy) NPs, including Ag:HfO_x, Ag:MgO, Ag:SiO_x, AgAu:SiO_2 or AgPt:SiO_2.[10,11]

https://doi.org/10.52326/ic-ecco.2021/EL.01

Typical memristive devices are metal-insulator-metal structures with the insulator thickness in the low nm range, mainly governed by the transport of metal cations or oxygen vacancies across the nm gap. In contrast, recently a particular research interest lies in massively parallel, self-organized structures, for example nanowire or NP networks at or beyond the percolation threshold.[13–17] Here, a common feature is that the dynamic transitions are found to be scale-invariant, with probabilities for resistance change, inter-spike interval, avalanche duration and avalanche size governed by power laws.[14,15] In many aspects the dynamic transitions show striking similarities to avalanche dynamics and long-range temporal correlations in neural systems.[14,18] For this reason, self-organized NP networks are considered as an interesting next-gen device candidate for reservoir computing and in neuromorphic engineering.

The close connection of sensing and processing, known from biological systems, has attracted increasing attention in material science and electrical engineering recently. Memristive devices have been combined with a variety of sensor devices to enable applications such as artificial skin or as optically modulated synapses.[19–22] Wide band gap transition metal oxides, such as TiO_2, are well known for their sensing capabilities towards photons (with sufficient photon energy to generate electron-hole pairs) and towards gas molecules (via adsorption of gas molecules on the sensor surface).[23–26] A promising approach to achieve distributed processing of the sensor information is to combine sensor elements with memristive devices, whose reconfigurable resistance serves as a means to pre-process the sensor data, e.g. by adaptation.[27]

In this work, the viability of NPs as building units for bio-inspired devices will be elucidated at the example of multistack memristive devices with diffusive memristive switching characteristics, as highly interconnected Ag NP networks and as TiO_2 NP assemblies with photon-sensitive resistance states.[1]

II. Materials and Methods

The fabrication of NP-based devices was realized by physical vapour deposition (PVD) processes in custom-build high vacuum (HV) deposition systems. NPs were deposited using gas phase synthesis approaches, namely magnetron-based Haberland-type gas aggregation source in case of the Ag NPs from metallic Ag target and alloy AgAu NPs via multicomponent target approach and supersonic cluster beam deposition from pulsed microplasma cluster source (PCMS), using a metallic Ti rod, in case of TiO_2 NPs.[28,29] Post deposition heat treatment was performed in an muffle furnace (controlled by PID Fuji Electric PXZ) at 600°C for 1h to safeguard complete oxidation of the Ti NPs. Details on the fabrication process are reported elsewhere.[10,30–32] To embed the metallic NPs and achieve a sparse arrangement of the AgAu NPs in the multistack devices, dielectric SiO_2 matrix was deposited by pulsed DC reactive magnetron sputtering.[10] Electrical characterization of lateral and horizontal NP arrangement was performed via a source measure unit (Keithley, 2400 Source Measure Unit; Agilent, E52790B). The contacting of multistack devices is reported in full details elsewhere[10]. Contacting of the Ag NP network device was done by a four point probe station (Signatone, H150W) with micromanipulators and conventional tungsten tips (Signatone, SE-T). Contacting of TiO_2 NP network sensors was achieved using custom-made positioners featuring spring contacts (SS-40-J-1.8-G-N/L D/C). To measure the electrical characteristics, DC voltage sweeps as well as constant voltage were applied and the current response of the respective device was recorded. On the basis of the IV-data, the resistance was estimated using Ohm's law. No electroforming steps were performed for the measurements.

III. Results and Discussion

In the AgAu NP multistack memristive device, the individual NPs are separated by a dielectric SiO_2 matrix, resulting in a sparse distribution of the metallic NPs within the matrix. For these devices, reproducible diffusive memristive switching is commonly observed and has been reported previously.[10] The main characteristic of memristive switching in these multistack devices is that the separation of the metallic NPs leads to an initially high electrical resistance. Upon application of a sufficiently high voltage, Ag atoms from the alloy NPs are ionized and transported alongside the electrical field. Following a reduction to metallic silver, a conductive metallic filament is formed, effectively bridging the dielectric matrix in the multistack device and substantially reducing the electrical resistance. Due to the limited availability of Ag species from the alloy NPs as well as the tendency to conserve surface energy, the metallic filaments are prone to spontaneous decay, resulting in the dissolution of the filament and consequently restoring of the initial high electrical resistance.[10,11]

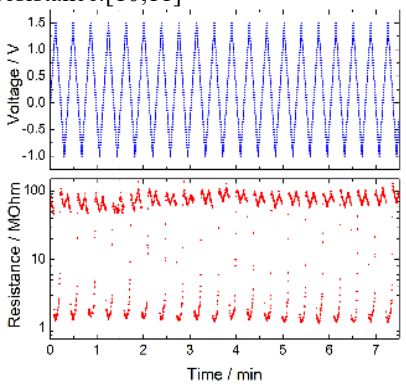

Figure 1. Resistance over time (bottom) for a AgAuNP multistack memristive device under application of a sawtooth voltage ramp (top)

[1] Funded by the Deutsche Forschungsgemeinschaft (DFG, German Research Foundation) – Project-ID 434434223 – SFB 1461 and Research Unit FOR 2093 and funded by the German Academic Exchange Service (DAAD).

https://doi.org/10.52326/ic-ecco.2021/EL.01

In case a sawtooth voltage is applied to the AgAu NP multistack device, commonly a IV hysteresis loop is recorded. In an alternative representation, the time dependent resistance response can be obtained from the recorded IV data (cf. Fig. 1). Here, the transitions between two distinct resistance states become immediately obvious. In Fig. 1, 20 consecutive switching cycles of a AgAu NP multistack device are depicted. For each cycle, the device switches between a low resistance state (LRS) and a high resistance state (HRS). There are only very few data points in between both resistance states, indicating that the switching is very fast compared to the data acquisition rate, which lies in the range of 100 ms in the presented measurement. From the *R vs t* data in Fig. 1, the resistance levels for the LRS and HRS state can be obtained. In the histogram (as depicted in Fig. 2) of the resistance states that are occupied within the operational window between 0.5V and 0.75V, a clear separation between the LRS and HRS can be observed. In case of this AgAu NP multistack device, a serial resistance of 1 MΩ was applied during the electrical characterization to limit the overall current.[10] This serial resistance dominates the LRS, while the HRS exhibits a resistance that is higher by more than one order of magnitude.

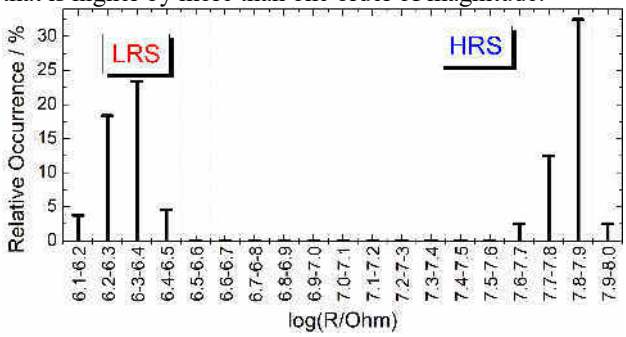

Figure 2. Histogram of resistance states in the diffusive siwtching window between 0.5V and 0.75V for a AgAuNP multistack memristive device

In addition to the AgAu NP multistack device with its sparse arrangement of NPs inside a dielectric matrix, another interesting device class using metallic NPs as building units are highly interconnected NP networks. To achieve such nanogranular assemblies, commonly surfactant-free gas phase synthesis methods such as the magnetron-based Haberland-type gas aggregation source [14] or the pulsed microplasma cluster source (PCMS) [15] are applied. In contrast to typical, predefined structural arrangements such as cross-bar arrays in the field of memristive devuces, the NP networks are deposited onto substrates in a lateral geometry, with two or more prestructured electrodes. The statistical nature of the deposition process and the low impact energy of the NPs that arrive at the substrate result in a random assembly of connections and resistive switching gaps between the NPs. A schematic snapshot of a NPs network between two contacts is shown in Fig. 3 (a). At this time of the deposition, there is a considerable number of open gaps between connected arrangements of NPs. Compared to the multistack NP devices, the sparseness of the NP arrangement is reduced with increasing deposition time. The more NPs are deposited onto the substrate, more and more NPs are in direct contact with each other, resulting in an increase in potential current paths. In Fig. 3 (middle) a schematic percolation curve, i.e. the dependency of the electrical resistance over the deposition time, is depicted. For an underpercolated arrangement of NPs (at low deposition time), a low number of connections between individual NPs is prevalent, resulting in a high number of gaps, schematically shown in Fig. 3 (a), which leads to a high resistance. In the later stages of the deposition, a fully connected network with a high number of parallel conduction pathways is present, resulting in a low electrical resistance. In the intermediate regime, when the gaps between individual NP arrangements become closed, drastic changes in the electrical resistance are present, corresponding to the steep slope in Fig. 3. A SEM micrograph of an Ag NP network close to the percolation threshold is depicted in Fig. 3 (b).

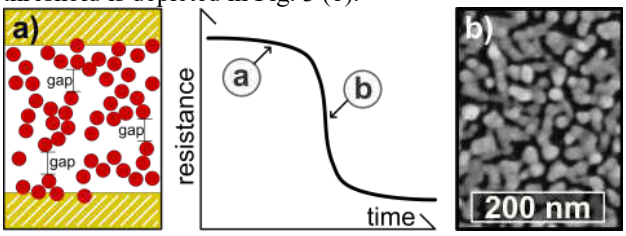

Figure 3. Typical *in-situ* measurement of the resistance in dependence of the lateral covering with NPs (middle). For low coverage, schematically shown in (a), a large amount of gaps between the NPs results in a large resistance. With increasing NP deposition, the onset of percolation goes alongside a steep slope, indicating the decrease in resistance, as shown for a SEM micrograph of a Ag NP network at percolation threshold (b).

In this work, NP networks of Ag NPs were fabricated via gas aggregation source and the electrical resistance was monitored during the deposition in order to obtain networks that fall into the intermediate regime (cf. Fig. 3 (b)). These highly interconnected networks of metal NPs are by no means limited to a purely linear ohmic I-V characteristic. In contrast, in nanogranular assemblies the high number of particle-particle interfaces and defects enables multiple resistance levels and dynamic transitions therein[15,33,34]. In Fig. 4 the time-dependent current response of an interconnected network of Ag NP is shown. Under application of a constant voltage, a rich transition between multiple resistance states can be observed. Each resistance state relates to a distinct configuration of the connectivity within the network, and the transition between two resistance states is mediated by local reconfigurations of Ag species from the Ag NPs. Similar to the limited lifetime of metallic filaments in the diffusive memristive devices, the transition between two resistance levels in the complex Ag network also underlies an intrinsic variability. Comparable electrical characteristics have been reported for a variety of NP

https://doi.org/10.52326/ic-ecco.2021/EL.01

networks, ranging from Sn/SnO_x NP networks[14] close to the percolation threshold to Au NP networks well above the percolation threshold.[15] This implies that the complex switching between a variety of resistance levels is inherently related to the nanogranular assembly and can be achieved by a variety of materials.

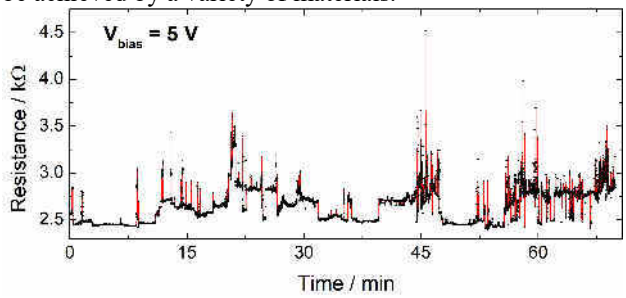

Figure 4. Resistance over time for 5 V applied to a AgNP network. In contrast to the individual diffusive switching in low dimensional NP arrangements, a high number of different resistance states is occupied.

The *R vs. t* measurement exhibits a high number of transitions between resistance states. To visualize the occurrence of the multitude of resistance states, the histogram corresponding to the time-dependent measurements at constant bias is depicted in Fig. 5. In contrast to the multistack NP device, here there is a spread of occupiable resistance states and no clear separation between distinct HRS and LRS can be observed. Notably, the network dynamics show separated periods of burst-like activity and periods of silence, which in many aspects resembles avalanche dynamics and long-range temporal correlations in neural systems.[14,18] For this reason, the electrical characteristics of self-organized NP networks makes them an interesting next-gen device candidate for neuromorphic engineering and reservoir computing, which requires interacting non-linear elements in a complex arrangement, able to map input information into temporal dynamics in the network.

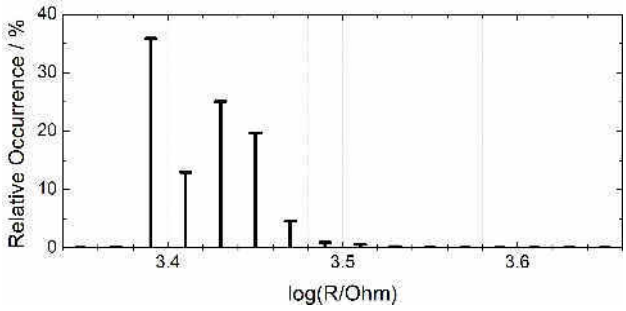

Figure 5. Histogram of the resistance states that are occupied in a AgNP network sample. Compared to the histogram of diffusive memristive switching in sparse AgAu NP arrangements, here a continous spectrum of occupieable resistance states is observed.

Nanogranular assemblies are by no means limited to noble metal NPs. In contrast, the extension of lateral NP networks towards transition metal oxide NPs opens up the potential for additional functionalities, for example sensing. As such, an interesting parallel to biological systems can be found, in which sensing and data processing are closely connected. With the junction of memristive switching and sensing it is possible to obtain accommodation to constant stimuli via adaptation.[27] An interesting application of NPs as functional building blocks in the field of sensing is the surface decoration of semiconducting metal oxide thin film sensors for gas sensing applications.[25] For semiconducting metal oxide gas sensors, the presence of metallic NPs at the sensor layer surface is commonly reported to result in a change in the sensitivity and selectivity of the sensor.[35–37]

In this section, the UV sensing properties of networks of TiO_2 NPs fabricated using supersonic cluster beam depositon from PCMS are discussed. The electrical response of a TiO_2 NP network between two Au electrodes (spacing 1mm) at a voltage bias of 10V is depicted in Fig. 6.

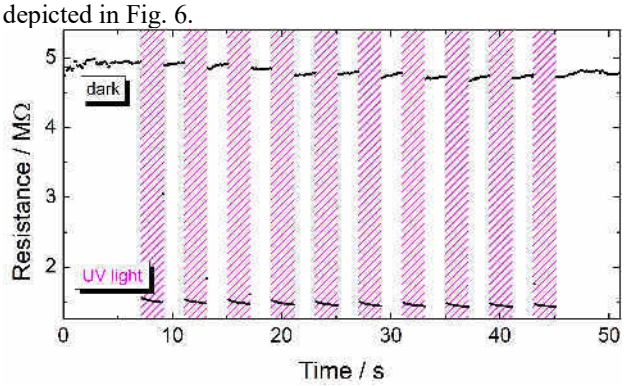

Figure 6. Resistance behaviour of a TiO_2 NP network, post-deposition heat treated for 1h at 600°C in air, UV illumination is applied in 10 pulses of 2s each (constant voltage of 10V applied).

While the resistance in the dark state (without illumination) lies in the range of 4.9 MΩ, the application of UV illumination (for 10 pulses with 2 s duration each) leads to a significant reduction in the resistance down to roughly 1.5 MΩ.

In analogy to the histograms of the resistance states in the multistack AgAu NP device and the Ag NP networks, the resistance states with and without UV illumination are depicted in the histogram in Fig. 7. Here, the clear separation between the dark and the illuminated state becomes clear. It has to be pointed out, that the resistance state "UV on" strongly depends on the illumination intensity.

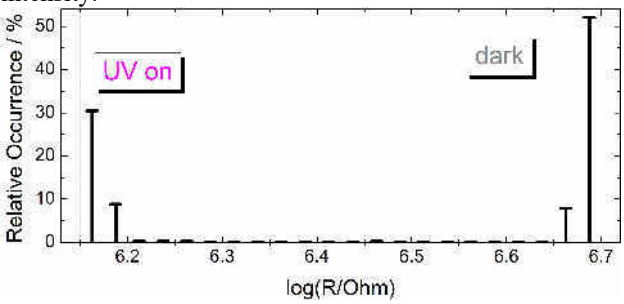

Figure 7. Histogram of the resistance states under illumination (UV on) and without illumination (dark)

https://doi.org/10.52326/ic-ecco.2021/EL.01

IV. CONCLUSION

NPs are promising functional bulding blocks for a variety of (nano)electronic devices. Three use cases for nanoparticular assemblies are discussed. The well-defined local confinement of memristive action due to the field enhancement between NPs and the limited reservoir of Ag-species in the AgAu alloy NPs results in reproducible diffusive memristive switching in sparse AuAu NP multistack devices with clearly separated resistance states. Dynamic transitions between multiple resistance states were observed in highly connected lateral Ag NP networks. Here, the high number of connections and interfaces enable complex behaviour and results in a plethora of accessible resistance states that do not show a clear separation like in the sparse AgAu NP multistack device. The usage of semiconducting metal oxide NPs, at the example of TiO_2 NPs, extends the usage of interconnected NP networks towards two-terminal sensor devices with well-separated illumination dependent resistance states. Owing to the broad application potential, nanogranular systems with NPs as their building units are a promising candidate for the development of bio-inspired computing architectures.

ACKNOWLEDGMENT

A.V., N.C. T.S. and F.F. would like to thank Stefan Rehders for technical assistance in the setup and operation of NP deposition via gas aggregation source. A.V. would like to thank Paolo Piseri, Gianluca Martini, Anita Previdi and Claudio Piazzoni for fruitful discussions on NP networks and the deposition of TiO_2 NPs from pulsed microplasma cluster source.

REFERENCES

[1] J. P. Crutchfield, W. L. Ditto, and S. Sinha, "Introduction to Focus Issue: Intrinsic and Designed Computation: Information Processing in Dynamical Systems—Beyond the Digital Hegemony," *Chaos* **20**, 037101 (2010).

[2] K.-P. Zauner, "From Prescriptive Programming of Solid-State Devices to Orchestrated Self-organisation of Informed Matter," in *Unconventional Programming Paradigms* **3566**, J.-P. Banâtre, P. Fradet, J.-L. Giavitto, and O. Michel, Eds. (Springer Berlin Heidelberg, Berlin, Heidelberg, 2005).

[3] J. D. Kendall and S. Kumar, "The building blocks of a brain-inspired computer," *Applied Physics Reviews* **7**, 011305 (2020).

[4] H. Yu, H. Wei, J. Gong, H. Han, M. Ma, Y. Wang, and W. Xu, "Evolution of Bio-Inspired Artificial Synapses: Materials, Structures, and Mechanisms," *Small* **17**, 2000041 (2021).

[5] C. D. Wright, "Precise computing with imprecise devices," *Nat Electron* **1**, 212–213 (2018).

[6] G. W. Burr, R. M. Shelby, A. Sebastian, S. Kim, S. Kim, S. Sidler, K. Virwani, M. Ishii, P. Narayanan, et al., "Neuromorphic computing using non-volatile memory," *Advances in Physics: X* **2**, 89–124 (2017).

[7] D. Ielmini, "Brain-inspired computing with resistive switching memory (RRAM): Devices, synapses and neural networks," *Microelectronic Engineering*, 10 (2018).

[8] A. Haj-Ali, R. Ben-Hur, N. Wald, R. Ronen, and S. Kvatinsky, "Not in Name Alone: A Memristive Memory Processing Unit for Real In-Memory Processing," *IEEE Micro* **38**, 13–21 (2018).

[9] B. J. Choi, A. C. Torrezan, K. J. Norris, F. Miao, J. P. Strachan, M.-X. Zhang, D. A. A. Ohlberg, N. P. Kobayashi, J. J. Yang, et al., "Electrical Performance and Scalability of Pt Dispersed SiO_2 Nanometallic Resistance Switch," *Nano Lett.* **13**, 3213–3217 (2013).

[10] A. Vahl, N. Carstens, T. Strunskus, F. Faupel, and A. Hassanien, "Diffusive Memristive Switching on the Nanoscale, from Individual Nanoparticles towards Scalable Nanocomposite Devices," *Sci Rep* **9**, 17367 (2019).

[11] Z. Wang, M. Rao, R. Midya, S. Joshi, H. Jiang, P. Lin, W. Song, S. Asapu, Y. Zhuo, et al., "Threshold Switching of Ag or Cu in Dielectrics: Materials, Mechanism, and Applications," *Advanced Functional Materials* **28**, 1704862 (2018).

[12] H. Jiang, D. Belkin, S. E. Savel'ev, S. Lin, Z. Wang, Y. Li, S. Joshi, R. Midya, C. Li, et al., "A novel true random number generator based on a stochastic diffusive memristor," *Nature Communications* **8**, 882 (2017).

[13] G. Milano, G. Pedretti, M. Fretto, L. Boarino, F. Benfenati, D. Ielmini, I. Valov, and C. Ricciardi, "Brain-Inspired Structural Plasticity through Reweighting and Rewiring in Multi-Terminal Self-Organizing Memristive Nanowire Networks," *Advanced Intelligent Systems* **2**, 2000096 (2020).

[14] J. B. Mallinson, S. Shirai, S. K. Acharya, S. K. Bose, E. Galli, and S. A. Brown, "Avalanches and criticality in self-organized nanoscale networks," *Sci. Adv.* **5**, eaaw8438 (2019).

[15] M. Mirigliano, D. Decastri, A. Pullia, D. Dellasega, A. Casu, A. Falqui, and P. Milani, "Complex electrical spiking activity in resistive switching nanostructured Au two-terminal devices," *Nanotechnology* **31**, 234001 (2020).

[16] A. Z. Stieg, A. V. Avizienis, H. O. Sillin, C. Martin-Olmos, M. Aono, and J. K. Gimzewski, "Emergent Criticality in Complex Turing B-Type Atomic Switch Networks," *Adv. Mater.*, 9 (2012).

[17] R. Zhu, J. Hochstetter, A. Loeffler, A. Diaz-Alvarez, T. Nakayama, J. T. Lizier, and Z. Kuncic, "Information dynamics in neuromorphic nanowire networks," *Sci Rep* **11**, 13047 (2021).

[18] N. Tomen, J. M. Herrmann, and U. Ernst, Eds., *The Functional Role of Critical Dynamics in Neural Systems* (Springer International Publishing, Cham, 2019).

[19] J. Wang, Z. Lv, X. Xing, X. Li, Y. Wang, M. Chen, G. Pang, F. Qian, Y. Zhou, et al., "Optically Modulated Threshold Switching in Core–Shell Quantum Dot Based Memristive Device," *Adv. Funct. Mater.* **30**, 1909114 (2020).

[20] D. Oller, R. Osgood, J. Xu, and G. E. Fernandes, "Optical rectification in a reconfigurable resistive switching filament," *Appl. Phys. Lett.* **115**, 043101 (2019).

[21] L. Zhou, S.-R. Zhang, J.-Q. Yang, J.-Y. Mao, Y. Ren, H. Shan, Z. Xu, Y. Zhou, and S.-T. Han, "A UV damage-sensing nociceptive device for bionic applications," *Nanoscale* **12**, 1484–1494 (2020).

[22] R. A. John, N. Yantara, M. R. Kulkarni, N. F. Jamaludin, J. Basu, S. G. Mhaisalkar, A. Basu, and N. Mathews, "Diffusive and Drift Halide Perovskite Memristive Barristors as Nociceptive and Synaptic Emulators for Neuromorphic Computing," *Adv. Mater.*, 13 (2021).

[23] A. Dey, "Semiconductor metal oxide gas sensors: A review," *Materials Science and Engineering: B* **229**, 206–217 (2018).

[24] W. Tian, H. Lu, and L. Li, "Nanoscale ultraviolet photodetectors based on onedimensional metal oxide nanostructures," *Nano Res.* **8**, 382–405 (2015).

[25] G. Korotcenkov, "Metal oxides for solid-state gas sensors: What determines our choice?," *Materials Science and Engineering: B* **139**, 1–23 (2007).

[26] A. Mirzaei, S. G. Leonardi, and G. Neri, "Detection of hazardous volatile organic compounds (VOCs) by metal oxide nanostructures-based gas sensors: A review," *Ceramics International* **42**, 15119–15141 (2016).

[27] A. Vahl, J. Carstensen, S. Kaps, O. Lupan, T. Strunskus, R. Adelung, and F. Faupel, "Concept and modelling of memsensors as two terminal devices with enhanced capabilities in neuromorphic engineering," *Sci Rep* **9**, 4361 (2019).

[28] K. Wegner, P. Piseri, H. V. Tafreshi, and P. Milani, "Cluster beam deposition: a tool for nanoscale science and technology," *J. Phys. D: Appl. Phys.* **39**, R439–R459 (2006).

[29] E. Barborini, P. Piseri, and P. Milani, "A pulsed microplasma source of high intensity supersonic carbon cluster beams," *J. Phys. D: Appl. Phys.* **32**, L105–L109 (1999).

https://doi.org/10.52326/ic-ecco.2021/EL.01

[30] A. Vahl, J. Strobel, W. Reichstein, O. Polonskyi, T. Strunskus, L. Kienle, and F. Faupel, "Single target sputter deposition of alloy nanoparticles with adjustable composition via a gas aggregation cluster source," *Nanotechnology* **28**, 175703 (2017).
[31] A. Podestà, F. Borghi, M. Indrieri, S. Bovio, C. Piazzoni, and P. Milani, "Nanomanufacturing of titania interfaces with controlled structural and functional properties by supersonic cluster beam deposition," *Journal of Applied Physics* **118**, 234309 (2015).
[32] J. Drewes, A. Vahl, N. Carstens, T. Strunskus, O. Polonskyi, and F. Faupel, "Enhancing composition control of alloy nanoparticles from gas aggregation source by in operando optical emission spectroscopy," *Plasma Process Polym* **18**, 2000208 (2021).
[33] M. Mirigliano, F. Borghi, A. Podestà, A. Antidormi, L. Colombo, and P. Milani, "Non-ohmic behavior and resistive switching of Au cluster-assembled films beyond the percolation threshold," *Nanoscale Adv.* **1**, 3119–3130 (2019).
[34] M. Mirigliano, S. Radice, A. Falqui, A. Casu, F. Cavaliere, and P. Milani, "Anomalous electrical conduction and negative temperature coefficient of resistance in nanostructured gold resistive switching films," *Sci Rep* **10**, 19613 (2020).
[35] A. Vahl, O. Lupan, D. Santos-Carballal, V. Postica, S. Hansen, H. Cavers, N. Wolff, M.-I. Terasa, M. Hoppe, et al., "Surface functionalization of ZnO:Ag columnar thin films with AgAu and AgPt bimetallic alloy nanoparticles as an efficient pathway for highly sensitive gas discrimination and early hazard detection in batteries," *J. Mater. Chem. A* **8**, 16246–16264 (2020).
[36] O. Lupan, N. Ababii, D. Santos-Carballal, M.-I. Terasa, N. Magariu, D. Zappa, E. Comini, T. Pauporté, L. Siebert, et al., "Tailoring the selectivity of ultralow-power heterojunction gas sensors by noble metal nanoparticle functionalization," *Nano Energy* **88**, 106241 (2021).
[37] A. Vahl, J. Dittmann, J. Jetter, S. Veziroglu, S. Shree, N. Ababii, O. Lupan, O. C. Aktas, T. Strunskus, et al., "The impact of O-2/Ar ratio on morphology and functional properties in reactive sputtering of metal oxide thin films," *Nanotechnology* **30**, 235603 (2019).